12-cm Magneto-Electrostatic Containment Mercury Ion Thruster Development

WILLIAM D. RAMSEY*
Electro-Optical Systems, Pasadena, Calif.

A 12-cm magneto-electrostatic containment ion thruster was adapted for mercury operation to determine if the low discharge chamber losses associated with the use of cesium in this thruster could also be realized with mercury. Adaptation included repositioning the strip anodes in the discharge chamber and substituting a mercury hollow cathode for the cesium cathode. The modified thruster is being tested with several electrode systems. Current data indicates that 90% mass utilization efficiency is achieved at discharge chamber losses of 155 to 160 ev/ion.

Introduction

ONE of the principal sources of inefficiency in conventional ion thrusters is the loss of discharge plasma ions and electrons to the thruster walls. The magneto-electrostatic containment (MESC) thruster permits a significant increase in efficiency by providing a boundary at the discharge chamber walls which reflects a large fraction of both ions and electrons approaching it. Ions are reflected by an electrostatic field at the boundary while electrons are reflected by a magnetic field.

The basic configuration of the magneto-electrostatic plasma containment boundary is shown in Fig. 1. The magnetic configuration is an array of magnetic pole strips where adjacent poles are of opposite polarity. All are backed with a common magnetically "soft" material and are maintained at the same potential as the thruster cathode. Between each pair of pole strips is an anode strip electrically isolated from the magnets.

Since the magnet poles are at cathode potential, they are negative with respect to the discharge plasma and thus retard electron losses to the poles. The anode strips are maintained at a potential a few volts positive with respect to the discharge plasma; the resulting electrostatic field retards ion losses to the boundary. The transverse magnetic field retards electron motion directly to the anode strips; electrons must diffuse by multiple collisions to the magnetic field line joining the pole edges in order to reach the anode strip. The position of the anode strips above the magnet poles affects both the ion and electron losses; raising the strip reflects ions more effectively but allows more electron losses. This position is an important parameter in optimizing thruster operation. Details of the magneto-electrostatic boundary theory and operation have been reported earlier and are available in Ref. 1.

Effectiveness of the MESC thruster concept was demonstrated by the development of a highly efficient cesium ion thruster. Tests of a 12 centimeter diameter thruster provided operation at 95% mass utilization efficiency at discharge chamber loss of only 90 ev per extracted ion. This was significantly better performance than had been reported previously Further details are available in Ref. 2.

Presented as Paper 71-692 at the AIAA 7th Propulsion Joint Specialist Conference, Salt Lake City, Utah, June 14-18, 1971; submitted September 19, 1971; revision received January 3, 1972. This paper is based on work performed at Electro-Optical Systems under the sponsorship of the International Telecommunications Satellite Consortium (INTELSAT). Any views expressed in this paper are not necessarily those of INTELSAT. The results reported are due to the efforts of many people who contributed advice, guidance and criticism. The author wishes to express his gratitude to R. C. Speiser, E. L. James, R. M. Worlock and J. Mahoney for their technical assistance and special thanks to Roy Oldham, the engineering specialist, who helped in the design and assembly of the test setups used in the program.

Index category: Electric and Advanced Space Propulsion

*Physicist. Member AIAA.

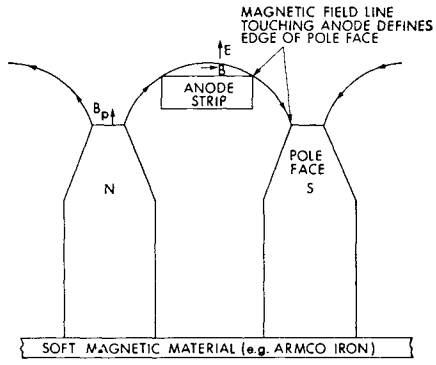

Fig. 1 Magneto-electrostatic containment geometry.

It was suggested that improved performance of mercury ion thrusters could also be achieved by the MESC thruster. This paper will discuss a program undertaken to explore the use of mercury in a 12 cm magneto-electrostatic containment ion thruster. This discussion will include a brief description of the modifications required to convert a cesium MESC thruster to mercury operation, and the type and kind of measurements and instrumentation used to evaluate thruster performance. The paper will conclude with a discussion of the thruster test results and the conclusions that can be drawn from these results.

Modification for Mercury Operation

To convert the 12 cm MESC thruster from cesium to mercury operation, a mercury hollow cathode subassembly had to be developed. The original cesium cathode was designed to operate at 500-600°C in a 15v discharge struck and maintained by the thruster anode. By contrast, a mercury hollow cathode operates at 1000-1400°C in a discharge struck and maintained by a keeper electrode and is located within a semi-enclosed region of the discharge chamber. The baffle structure, which forms the semi-enclosed region, divides the discharge into two zones: a high pressure region around the cathode which operates at 5-15v positive with respect to the cathode, and the main discharge which operates at 30-40v (Ref 3 and 4). The division in the discharge serves to reduce cathode erosion that would result from cathode operation in a 30-40v discharge and allows cathode "spot mode" operation at lower cathode propellant flow rates than would otherwise be possible.

The subassembly that evolved from the cathode development effort incorporates several interesting design features. For example, as shown in Fig. 2, rather than attach the cathode heater to the outside of the cathode structure, the heater was

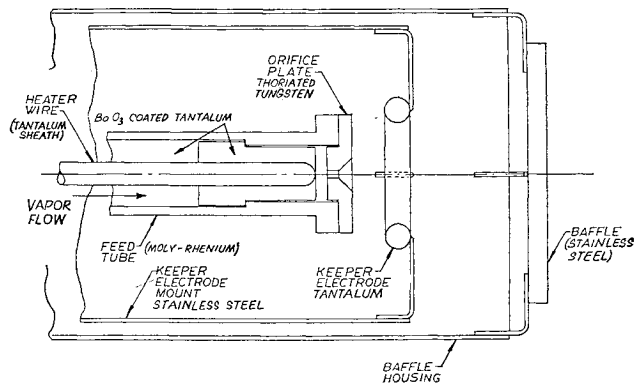

Fig. 2 Mercury hollow cathode for MESC thruster.

placed inside the delivery tube. This served to reduce cathode power and allowed the cathode subassembly to fit into the cathode magnetic pole piece. A 5.1 mm diameter internally heated cathode required 15 w to preheat to operating temperature and 2.5 w to sustain operation once the discharge was initiated. Final dimensions were those found to produce best thruster performance. The orifice plate was 5.1 mm in diameter with a 0.42 mm diameter orifice countersunk 0.5 mm on the downstream side. The keeper electrode was formed from a 1.0 mm diameter tantalum wire bent into a ring 4.3 mm inside diameter. Optimum position of the cathode subassembly in the discharge chamber was determined during thruster tests.

Measurements and Instrumentation

To evaluate thruster performance it is necessary to know the discharge power, the ion beam current, and the mass utilization efficiency. To determine the latter quantity it is necessary to know not only the propellant flow through the thruster and the resultant ion beam current but the ionization state of the ions in the beam. In the case of mercury, the assumption that all ions produced in the discharge are singly charged is unjustified due to the relatively small difference between mercury's first and second ionization potentials.

To determine the distribution of singly and doubly charged ions, time-of-flight data was collected as a part of thruster performance mapping. Experimental results are shown in Fig. 3; doubly charged ion production is plotted as a function of discharge voltage and corresponding data from the literature (Refs. 5 and 6) is shown for comparison. The experimental data shown was used in the reduction of thruster test data.

Two physically separate and electrically isolated feed systems were assembled to control and measure the mercury flow to the thruster. The dual feed system design was dictated by the need for independent control of propellant flow to the cathode and main feed ring and by the fact that the cathode feed operates at cathode potential while the main feed operates at anode potential. Each feed system consists of three sections: reservoir, flow meter, and vaporizer. Mass flow measurements are taken by valving off the reservoir and measuring the time required for the mercury level to drop a known distance in the capillary tube. Since the capillary diameter is known, the mercury flow rate can be calculated.

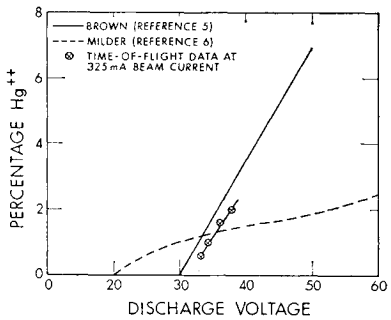

Fig. 3 Doubly charged ion production discharge voltage.

Experimental Operation and Results

For the purpose of discussion, thruster testing can be divided into four separate phases which explored the effect of selected physical changes in the thruster upon performance. The first test series determined the cathode subassembly position in the discharge chamber which produced maximum thruster efficiency (minimum ev/ion). The second series was undertaken to find the anode array height (position relative to the magnet pole strips) that produced a stable discharge at minimum ev/ion. The third test series determined size and position of the cathode baffle relative to the cathode keeper electrode which produced the optimum voltage-current discharge characteristics. The fourth and final series determined the effect of changing screen electrode transparency upon thruster performance. Experimental procedures and the results of each testing phase will be discussed below. A schematic of the MESC thruster used in testing is shown in Fig. 4.

To find the cathode position which produced minimum ev/ion, the cathode subassembly was mounted to a metal slide which could be moved from outside the vacuum chamber without disturbing thruster operation. The slide was mounted so its movement caused cathode subassembly movement along the discharge chamber axis.

Test results indicated best thruster performance was obtained when the cathode was located 1.6 mm downstream from the face of the cathode pole piece. This position corresponds approximately to the location of the maximum axial magnetic field. If the cathode assembly was moved upstream from this position, closer to the rear wall of the discharge chamber, the discharge became unstable and susceptible to easy extinction by any perturbation such as a spark in the electrode gap. If the cathode was located further than 1.6 mm into the discharge the ev/ion value increased. The discharge

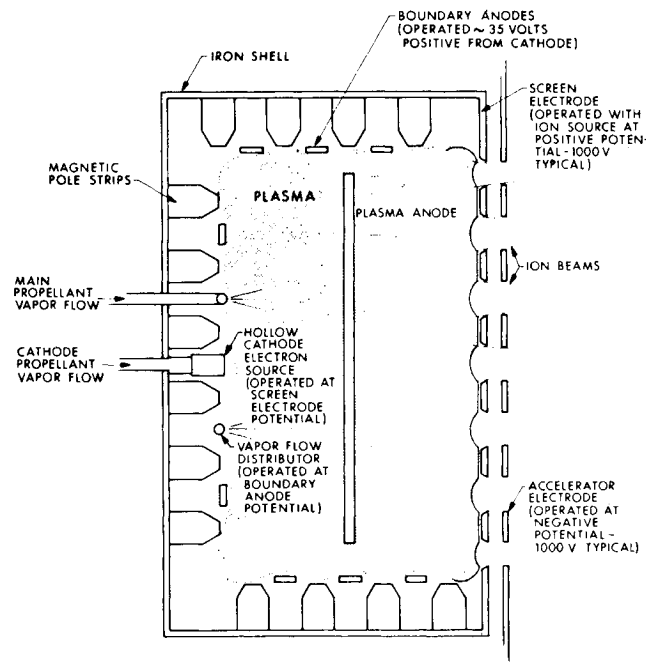

Fig. 4 MESC thruster schematic.

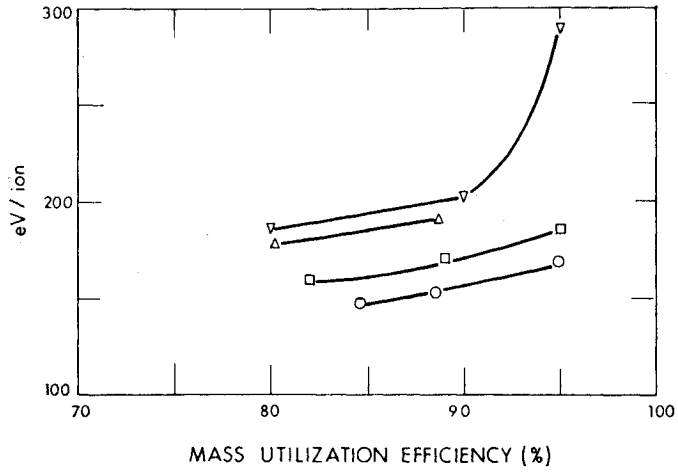

Fig. 5 Discharge power as a function of utilization efficiency.

instability probably resulted from a main discharge-cathode "decoupling" when the cathode was located upstream of the magnetic field maximum. Locating the cathode subassembly deeper than 1.6 mm in the discharge chamber placed the cathode too far downstream relative to the magnetic field maximum. All subsequent tests were conducted with the cathode located 1.6 mm downstream from the cathode pole face.

The initial position of the anodes in the discharge chamber was determined from the model developed in Ref. 2. The calculated location was 5.8 mm above the magnet pole faces. Tests conducted with the anodes in this location displayed symptoms of unstable discharge operation. Increasing the height from 5.8 to 6.4 mm produced stable operation and a reduction in discharge chamber ev/ion. Increasing the height further to 6.6 mm resulted in an increase in discharge power necessary to achieve a given mass utilization efficiency. The reduction in discharge power observed at 6.4 mm probably resulted from a reduction in ion recombination losses at the magnet pole faces, while the further increase in height resulted in too many electrons being collected by the anode array. Subsequent tests were conducted with the anodes at the 6.4 mm position.

Three physical dimensions directly affect the function of the cathode baffle structure in thruster operation: the distance between the keeper electrode and the baffle disk, the distance between the baffle support tube and baffle disk, and the diameter of the baffle disk (Fig. 2). In order to determine what baffle dimensions produced most efficient thruster operation, a series of tests was conducted in which the dimensions could be systematically varied. This was accomplished by attaching the baffle mounting tube to the metal slide used in the cathode positioning tests described above. Baffle disks of three different diameters were tested at different keeper electrode-to-disk gaps during thruster operation. The baffle diameters used were 71, 78, and 85% of the 1.4 cm inside diameter of the baffle support tube. The disk-to-support tube gap was varied from parallel with the end of the tube to 1.5 mm downstream in 0.5 mm increments during the testing of each disk.

Best over-all thruster performance was achieved with a keeper electrode-to-baffle gap of 4.8 mm and a support tube to baffle disk gap of 0.5 mm. Use of a baffle structure more restrictive than this, i.e., smaller tube-to-disk gap and/or smaller keeper-to-disk gap, made it necessary to use a higher cathode propellant flow in order to produce the same discharge v-I characteristics. Use of a more open baffle system required a high cathode propellant flow to maintain "spot mode" operation.

Thruster tests were conducted using two different sets of electrodes. Each electrode system was tested using two screen electrodes of 64 and 73% geometric transparencies. This was accomplished by testing each system before and after chemically milling the screen electrode. The electrode systems differed from one another only in number of apertures; one system contained 2269 while the other contained 2437. Each system was composed of a hexagonal array of 2.144 mm and 1.90 mm diameter apertures located on 2.540 mm centers. Chemical milling increased screen aperture diameter from 2.144 to 2.290 mm.

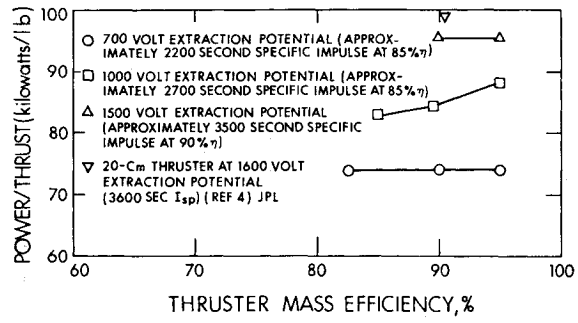

Fig. 6 Power/thrust vs mass utilization efficiency.

Data taken from the tests with all four electrode systems indicated the ev/ion necessary to achieve a given mass utilization efficiency decreased as the screen electrode transparency increased. The minimum ev/ion was achieved with the 2269 aperture electrode with 73% transparency.

The optimal ev/ion and power-to-thrust performance achieved during the MESC thruster tests are plotted against the mass utilization efficiency (corrected for Hg^{++}) in Fig. 5 and 6. The ev/ion value used in Table 1 and Figure 5 were derived from the ion beam current and the power consumed by the discharge (total power into discharge chamber except for cathode power). Calculation of the power-to-thrust ratio in Figure 6 included the power consumed by main vaporizer heater, cathode vaporizer heater, cathode heater, keeper electrode, discharge chamber power, beam current, and accelerator drain current.

Conclusion

The test results demonstrate the achievement of 148 ev/ion at 85% mass utilization and 160 ev/ion at 90% mass utilization. Although this represents an improvement on the published data with which the MESC performance results are compared, it does not represent the minimum ev/ion possible with the MESC design.

The 12 cm thruster used in this program was the first MESC thruster built. It is reasonable to assume that second and third generation designs will produce even better performance.

Table 1 Mercury MESC thruster, 2269 aperture electrode system 73% transparency

High voltage Positive		High voltage Negative		Boundary anode		Keeper		%	Adjusted[a] mass			Propellant equivalent mass
V+	I+	v−	I−	v	I	v	I	Hg++	efficiency	ev/ion	$(I_D-I_B)/I_B$	flow
(v)	(ma)	(v)	(ma)	(v)	(a)	(v)	(a)	(%)	(%)			(ma)
700	310	700	0.7	35	1.65	5.0	0.265	1.0	95.0	186	4.32	325
700	292	700	1.0	35	1.42	5.0	0.265	1.0	89.0	170	3.90	325
700	270	700	1.2	35	1.22	5.0	0.265	1.0	82.0	158	3.52	325
1000	310	900	1.0	34	1.51	5.0	0.265	0.7	95.0	167	3.87	325
1000	290	900	1.2	34	1.30	5.0	0.265	0.7	88.6	154	3.48	325
1000	277	900	1.5	34	1.20	5.0	0.265	0.7	84.7	148	3.33	325
1500	306	700	0.7	34	1.48	5.0	0.265	0.7	93.6	163	3.84	325
1500	290	700	1.0	35	1.22	5.0	0.265	1.0	88.3	147	3.21	325

[a] Thruster data has been corrected for the presence of doubly charged ions in the beam. Values shown represent the percentage of mercury mass flow which is ionized.

A number of areas of investigation could logically be pursued in continuing the development of the mercury MESC thruster.

One of the first areas of investigation would be the geometrical configuration of the discharge chamber. The original discharge chamber is a right hexagonal cylinder. It has a length-to-diameter ratio of one with an exposed magnetic pole face surface of 36 cm². The web surface area of the 73% transparent 2269 aperture screen electrode is approximately 37 cm², giving a total area of 73 cm² available for surface loss of ions. If the discharge chamber configuration is changed to an oblate spheroid with length-to-diameter ratio of 0.4, surface loss area will be decreased by approximately 10%.

Another area of investigation is screen grid transparency since the web area of the screen is one of the principal areas of loss. Higher transparency could be obtained by further machining of the existing design electrode although this would result in a rather delicate component. Higher transparency could also be obtained by the use of the composite grid structure in which the screen and accelerator electrode are replaced by a single metal-insulator bonded structure. Quite high transparency can be achieved by this approach. It is clearly worth further investigation since the achievement of 100% transparency would reduce surface loss area by an additional 22%. Although it has not been established that discharge losses vary linearly with surface loss area, it is reasonable to assume that the modifications mentioned would result in significant efficiency improvements.

References

[1] Moore, R. D., et al, "Cesium Electron Bombardment Thruster Research," Report 7240-Final, Contract NAS7-587, Oct. 1968, Electro-Optical Systems, Pasadena, Calif.

[2] Moore R. D., "Magneto-Electrostatically Contained Plasma Ion Thruster," AIAA Paper 69-260, Williamsburg, Va, 1969.

[3] King, H. J. and Poeschel, R. L., "Low Specific Impulse Ion Engine," CR-72677, 1970, NASA.

[4] Pawlik, E. V. and Fitzgerald, D. J., "Cathode and Ion Chamber Investigations on a 20-cm Diameter Hollow Cathode Ion Thruster," AIAA Paper 71-158, New York, 1971.

[5] Brown, S. C., *Basic Data of Plasma Physics*, Wiley, New York, 1961, p. 103–122.

[6] Milder, N. L., "Comparative Measurements of Singly and Doubly Ionized Mercury Produced by Electron Bombardment Ion Engine," TND-1219, July 1962, NASA.

[7] Knauer, W. and Poeschel, R. L., "The Radial Field Kaufman Thruster," *Journal of Spacecraft and Rockets*, Vol. 7, No. 3, March 1970, pp. 248–251.